International Journal of Computational and Experimental Science and ENgineering (IJCESEN)

Vol. 10-No.3 (2024) pp. 470-479
http://www.ijcesen.com

ISSN: 2149-9144

Research Article

Exploring gamma-ray and neutron attenuation properties of some high-density alloy samples through MCNP Monte Carlo code

Duygu SEN BAYKAL [1], Ghada ALMISNED [2], Hessa ALKARRANI [3,4], H.O. TEKIN [5,6,7*]

[1] Istanbul Nisantasi University, Faculty of Engineering and Architecture, Mechatronics Eng., Istanbul, Türkiye
Email: duygu.senbaykal@nisantasi.edu.tr - **ORCID:** 0000-0001-9833-9392

[2] Department of Physics, College of Science, Princess Nourah Bint Abdulrahman University, P.O. Box 84428, Riyadh, 11671, Saudi Arabia
Email: gaalmisned@pnu.edu.sa - **ORCID:** 0000-0001-9072-4480

[3] Research Institute for Medical and Health Sciences, University of Sharjah, Sharjah, 27272, Sharjah, United Arab Emirates
[4] Department of Medical Diagnostic Imaging, College of Health Sciences, University of Sharjah, 27272, Sharjah, United Arab Emirates
Email: halkarrani@sharjah.ac.ae - **ORCID:** 0009-0001-7823-5892

[5] Department of Medical Diagnostic Imaging, College of Health Sciences, University of Sharjah, 27272, Sharjah, United Arab Emirates
[6] Istinye University, Faculty of Engineering and Natural Sciences, Computer Engineering Dep., Istanbul, Türkiye
[7] Department of Physics and Technical Sciences, Western Caspian University, Baku, Azarbaijan
* **Corresponding Author Email:** htekin@sharjah.ac.ae - **ORCID:** 0000-0002-0997-3488

Article Info:

DOI: 10.22399/ijcesen.422
Received : 16 August 2024
Accepted : 05 September 2024

Keywords :

Alloy Compositions
Shielding Parameters
Phy-X/PSD
MCNPX

Abstract:

Effective radiation shielding is critical across various sectors, including nuclear power generation and medical applications. This study evaluates the radiation attenuation properties of seven distinct alloy samples: 316 Stainless Steel, Zircaloy-4, Monel 400, Alloy 625, Titanium Grade-5 (Ti-6Al-4V), Niobium-Titanium (NbTi) Alloy, and Haynes 230. Using the MCNP Monte Carlo simulation code and the Phy-X/PSD software, the gamma and neutron shielding capacities of these alloys were systematically investigated. Among the alloys, Haynes 230 exhibited superior gamma radiation attenuation efficiency. Furthermore, the Fast Neutron Removal Cross Section (FNRCS) values indicated that Haynes 230 (0.16375 1/cm) possessed comparable neutron shielding capabilities to 316 Stainless Steel (0.16758 1/cm) and Monel 400 (0.16818 1/cm), underscoring its robustness as a neutron shield. Although Monel 400 and 316 Stainless Steel demonstrated marginally better neutron shielding performance, Haynes 230 remains a formidable contender due to its balanced performance against both gamma and neutron radiation, making it a promising candidate for applications requiring comprehensive radiation protection. Moreover, the study demonstrated that Haynes 230 exhibited a significant advantage in terms of its linear attenuation coefficient, HVL, TVL, and mean free path (mfp) values, further solidifying its role as an efficient gamma-ray shield. Additionally, Monte Carlo simulations highlighted the superior transmission factor (TF) of Haynes 230, especially for thicker materials, positioning it as an ideal material for high-intensity radiation shielding applications.

1. Introduction

The selection of materials is essential in the field of radiation shielding to ensure both safety and efficiency [1]. Alloys are commonly preferred in this situation because of their distinctive blend of robustness, resistance to corrosion, and capability to reduce various forms of radiation [2]. 316 stainless steel is highly regarded for its exceptional corrosion resistance, which makes it essential in conditions where chemical stability is of utmost importance. Zircaloy-4 is primarily utilized in nuclear reactors

because of its favorable characteristics, including a low neutron absorption cross-section and excellent resistance to corrosion in hot water settings. Monel 400, a nickel-copper alloy, is renowned for its remarkable corrosion resistance, even in the presence of very aggressive chemicals. Alloy 625, a superalloy made primarily of nickel, possesses exceptional resistance to both high temperatures and corrosive conditions, all while retaining its impressive tensile strength. Titanium Grade-5 (Ti-6Al-4V), commonly referred to as the mainstay of the titanium sector, provides a remarkable equilibrium between durability and mass. Niobium-titanium (NbTi) alloy is often used to make superconducting magnets because it has a unique combination of being strong mechanically and superconducting at low temperatures. Haynes 230 is a high-performance alloy composed of nickel, chromium, tungsten, and molybdenum. It demonstrates exceptional resistance to oxidation and maintains its stability under high-temperature conditions [3-9]. The Phy-X/PSD software was used to find out how well these alloys blocked radiation [10]. This software is a reliable tool for finding important shielding metrics like mass attenuation coefficients, effective atomic numbers, and electron densities. These metrics offer crucial insights into the ability of each alloy to reduce certain types of ionizing radiation. In addition, the study employed the Monte Carlo MCNP code, a widely recognized modeling tool, to calculate the gamma-ray transmission factors for each alloy. The MCNP code accurately predicts transmission factors by modeling the interactions of gamma photons with materials. These transmission factors are crucial for determining the amount of radiation that goes through a specific thickness of material [11-15].

2. Material and Methods

2.1 Shielding Parameters

Understanding how gamma rays are attenuated as they pass through a material is crucial in radiation studies. The relationship between the attenuated gamma rays I(x) and the initial unattenuated gamma rays $I_0(x)$ is described by the linear attenuation coefficient (μ), which represents the probability of gamma rays being absorbed or scattered per unit thickness of the material, measured in cm^{-1} [16-17].

$$I(x) = I_0 e^{-\mu x} \quad (1)$$

The mass attenuation coefficient ($\mu_m = \mu/\rho$) is used to normalize the linear attenuation coefficient by the material's density (ρ), making it a key parameter for comparing the radiation absorption properties of different materials. The half-value layer (HVL) is the thickness of a material required to reduce the intensity of gamma rays by the half. It is calculated using the linear attenuation coefficient as [16-17]:

$$HVL = \frac{ln(2)}{\mu} \quad (2)$$

This parameter is essential for evaluating a material's effectiveness in shielding against radiation. The tenth-value layer (TVL) is the thickness needed to reduce the intensity of gamma rays by a factor of ten. It is calculated similarly [16-17]:

$$\text{TVL} = \frac{ln(10)}{\mu} \quad (3)$$

TVL is particularly important in scenarios requiring more stringent radiation protection. The mean free path (MFP) is the average distance that a gamma-ray photon travels in a material before interacting. It is inversely related to the linear attenuation coefficient [16-17]:

$$\text{mfp} = 1/\mu \quad (4)$$

This concept helps assess how effectively a material can slow down or stop gamma rays. In composite materials, the effective atomic number (Z_{eff}) plays a crucial role, particularly in Compton scattering interactions. It is calculated using the total and electronic cross-sections (σ_T and σ_e) and helps in understanding the material's interaction with radiation [16-17].

$$Z_{eff} = \frac{\sigma_T}{\sigma_e} \quad (5)$$

The effective electron density (N_{eff}) is another important parameter that describes the electron density available for interaction with gamma rays in a material, influencing the scattering and absorption processes. Finally, the fast neutron effective removal cross-section (Σ_R) is vital in environments with significant neutron exposure, such as nuclear reactors. It indicates how effective a material is at reducing the intensity of fast neutrons, with higher values representing better shielding capabilities [18-19]. All these radiation shielding factors were analyzed using the Phy-X/PSD program, which allows for precise simulations of various alloy compositions and thicknesses, providing a detailed understanding of how different materials perform in radiation shielding applications.

2.2 MCNP Monte Carlo Simulations

Evaluating the efficacy of shielding materials in reducing the intensity of gamma rays, namely

primary and secondary gamma rays, is crucial. Having a comprehensive understanding of the underlying characteristics of gamma ray shielding is quite important. The transmission factor (TF) is an important measure that demonstrates the ability of materials to reduce the intensity of ionizing gamma rays [20]. The study used the MCNP Monte Carlo simulation program, specifically version 2.7.0, to calculate the transmission factor (TF) for the alloy materials under investigation. The transmission factor (TF) measures the proportion of gamma ray flux that is able to pass through a substance compared to the flux that first reaches the surface of the material. This ratio is computed for every individual element. To do this calculation, the average gamma ray intensity detected in the F4 tally mesh was divided by the average gamma ray intensity recorded in a uniform detection region [21]. The computation was conducted using the MCNP code, with two detection fields placed: one in front of the alloy to measure the intensity of the primary gamma rays entering the material, and another behind the alloy to measure the intensity of the gamma rays that had passed through the material [22]. Figure 1 illustrates the MCNP simulation setup used for computing the transmission factor. The simulation's input file consists of three main components: the cell, the surface, and the data card. The transmission factor was calculated by assessing the geometric parameters obtained from the input file. Initially, the cell formations were quantified in order to accurately determine their surface areas and densities. Afterwards, the exact arrangement of the surfaces for the layout of the transmission factor was established. The energy of the radioisotopes and the shape of the source were entered into the data card section during the final step. The original geometry was generated as a singular point releasing radiation uniformly in all directions with consistent characteristics.

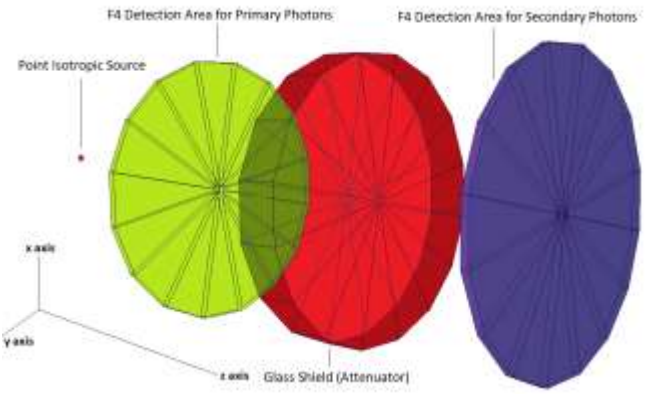

Figure 1. *3-D illustrations of designed MCNP simulation setup.*

3. Results and Discussions

The objective of this research was to determine the effectiveness of several materials, including 316 Stainless Steel, Zircaloy-4, Monel 400, Alloy 625, Titanium Grade-5 (Ti-6Al-4V), Niobium-Titanium (NbTi) Alloy, and Haynes 230, in blocking radiation over a broad spectrum of temperatures and energies. The energy of radiation is significantly reduced by two factors: the density of the substance and the atomic structure of the material [23-27]. Figure 2 clearly displays the density values of the studied alloys.

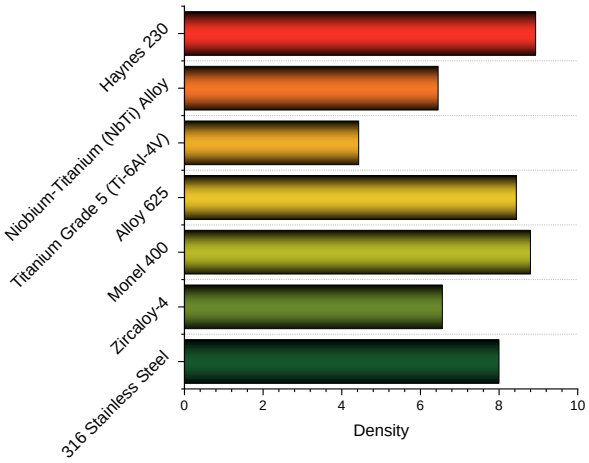

Figure 2. *Density variation of investigated alloys.*

Figure 3 displays the linear attenuation coefficient, which represents the rate at which radiation intensity decreases per unit thickness. Furthermore, this graphic also illustrates the mass attenuation coefficient, which quantifies the ability of a material to block radiation regardless of its density. Based on the comparative results, Haynes 230 had the highest value among the examined alloys. Conversely, Zircaloy-4 had a greater MAC value, with Haynes 230 closely behind as the second most esteemed alloy. Figure 4 displays the HVL and TVL parameters. These metrics represent the minimum thickness of the material required to decrease the radiation intensity to 50% and 10% of its original value. The data indicate that Haynes 230 exhibits the lowest values, indicating that the distance over which radiation may propagate through Haynes 230 decreases as the energy level increases [28-32]. Figure 5 displays the mean free path (mfp) parameter, which quantifies the average distance that a photon may travel through a material without interacting with it. Haynes 230 also has the minimum value for this parameter. Some people call the fast neutron removal cross section (FNRCS) an important number that shows how well a material gets rid of or absorbs fast neutrons through different

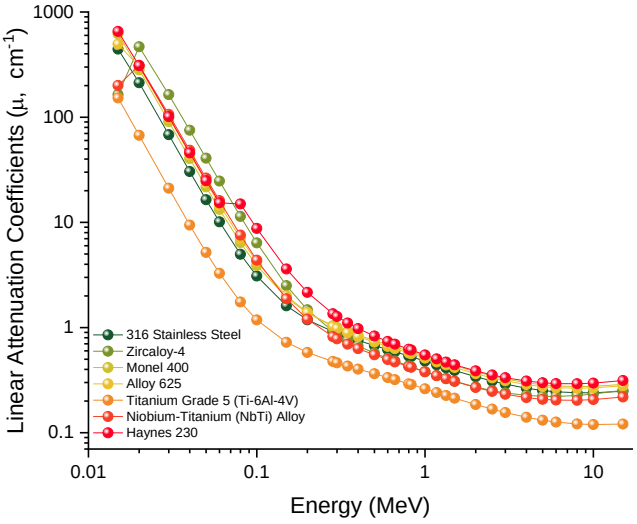

(a)

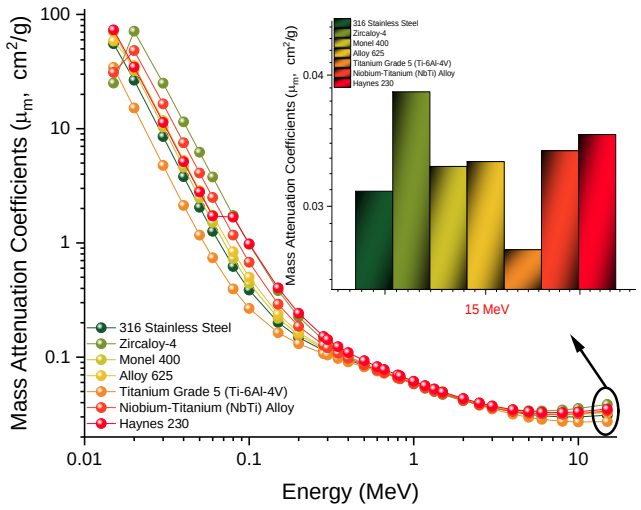

(b)

Figure 3. *Variation of (a) linear attenuation coefficient (cm^{-1}) with photon energy (MeV) and (b) mass attenuation coefficients (cm^2/g)for all investigated alloy types.*

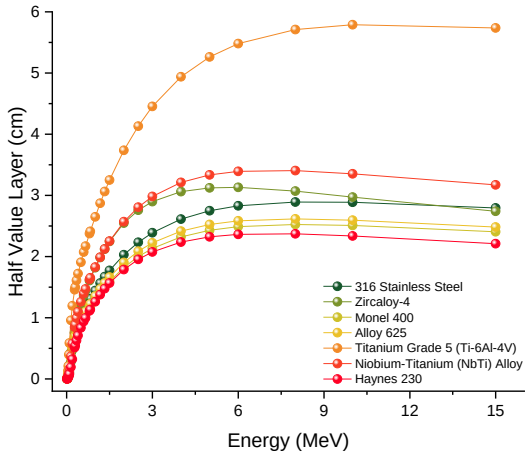

(a)

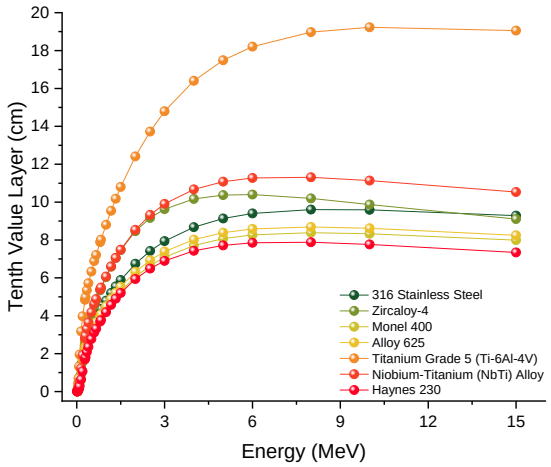

(b)

Figure 4. *Variation of the half-value layer (cm) and the tenth-value layer (cm) with photon energy (MeV) for all investigated alloy types.*

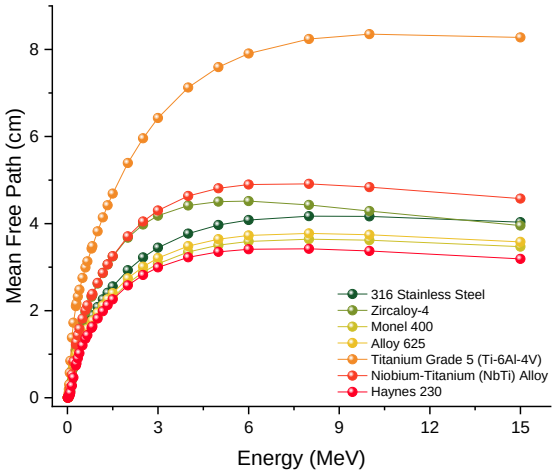

Figure 5. *Variation of mean free path (cm) with photon energy (MeV) for all investigated alloy types.*

interactions, such as scattering or absorption. The FNRCS values for the examined alloys are shown in Figure 6. Haynes 230, like 316 stainless steel (0.16758 1/cm) and Monel 400 (0.16818 1/cm), shown notable effectiveness in shielding against neutrons with a surface area of 0.16375 1/cm. The performance of this material was similar to that of both of these materials. When assessing the suitability of a material for gamma-ray applications, it is important to take into account the effective atomic number (Z_{eff}) as a key measure. This number is associated with the material's ability to attenuate the intensity of gamma rays [33-40]. Similar results have been obtained in previous studies [41-47]. Figure 7 displays the Z_{eff} values of the alloys as they vary with photon energy. Figure 8 illustrates a linear correlation between the effective atomic number and the number of electrons (N_{eff}). Both figures are shown as three-dimensional objects. Figure 9 illustrates the relationship between energy and exposure buildup factor (EBF) for different mean

free path (mfp) values. Chemical reactions occurring in different natural contexts show that elements with large atomic

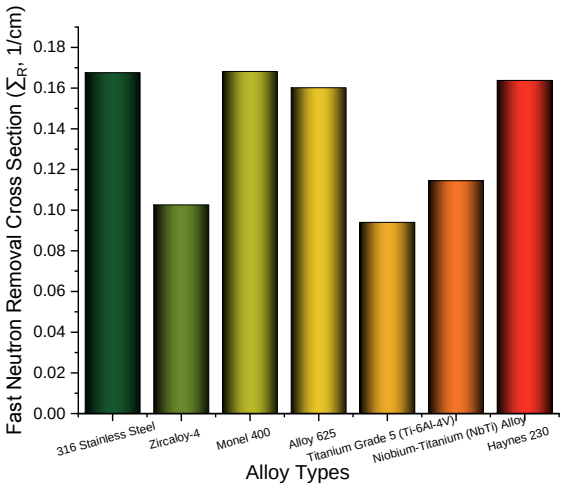

***Figure 6**. Variation of fast neutron removal cross section (∑R, 1/cm) values of all investigated alloy types.*

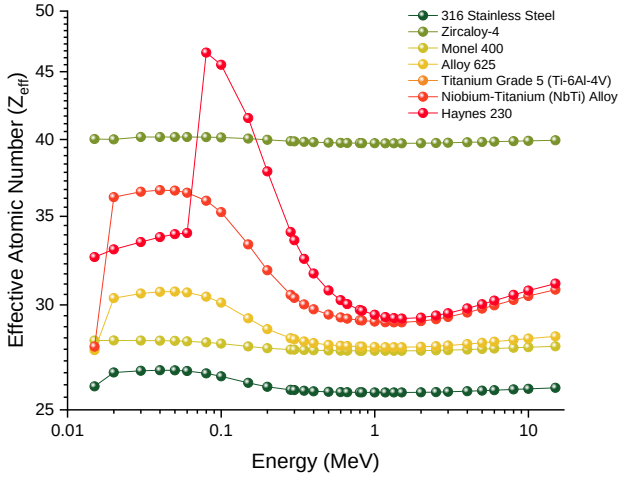

***Figure 7.** Variation of effective atomic number (Z_{eff}) with photon energy (MeV) for all investigated alloy types.*

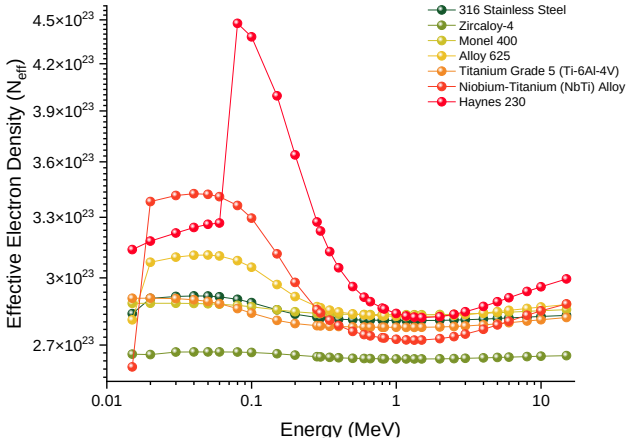

***Figure 8.** Variation of effective electron density (N_{eff}, electrons/g) with photon energy (MeV) for all investigated alloy types.*

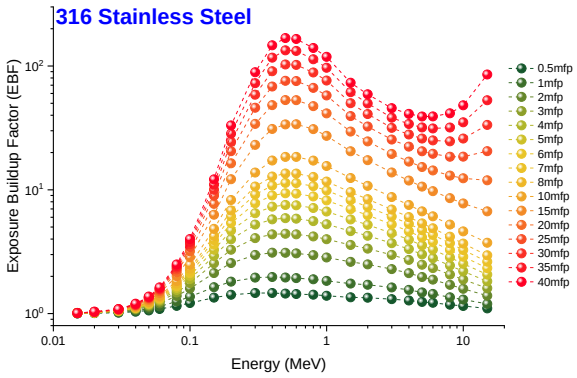

(a)

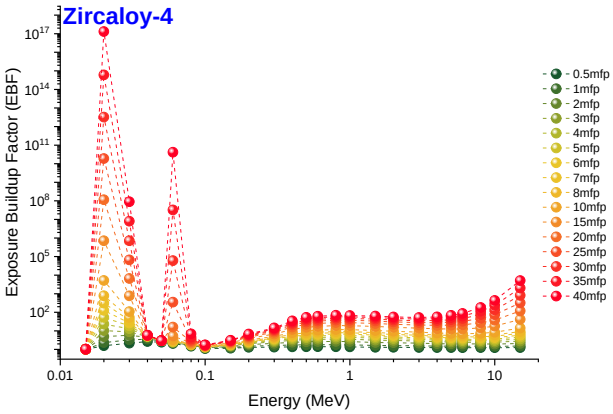

(b)

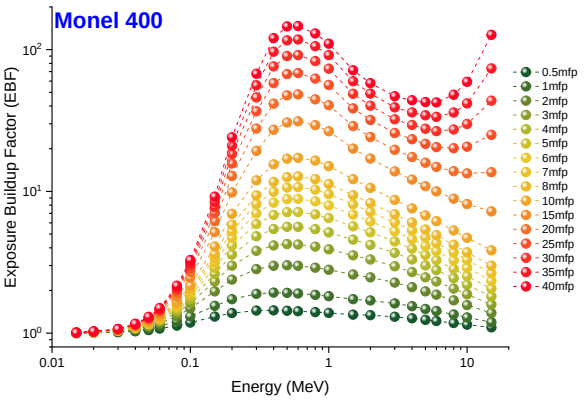

(c)

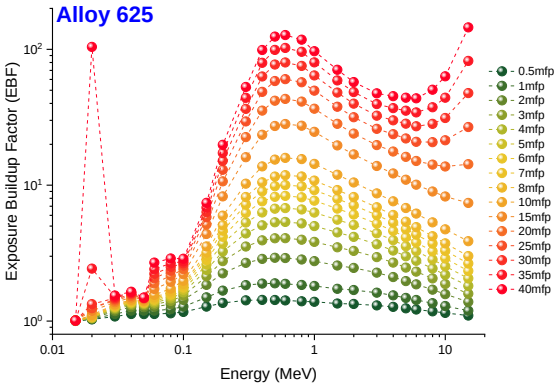

(d)

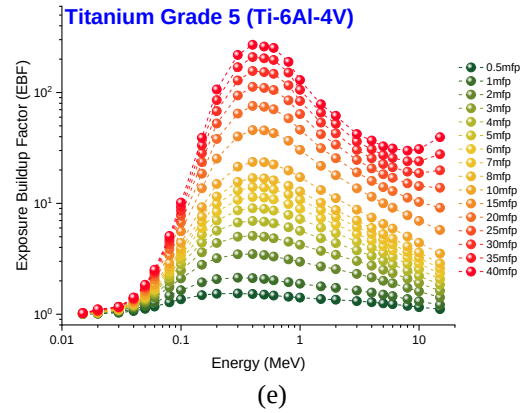

(e)

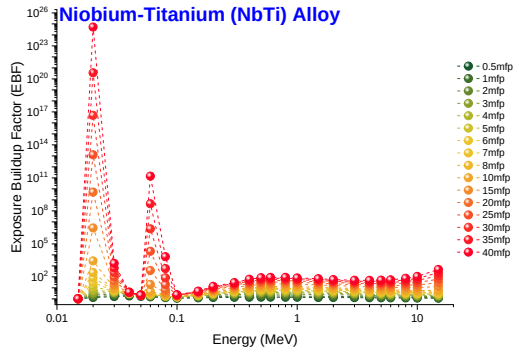

(f)

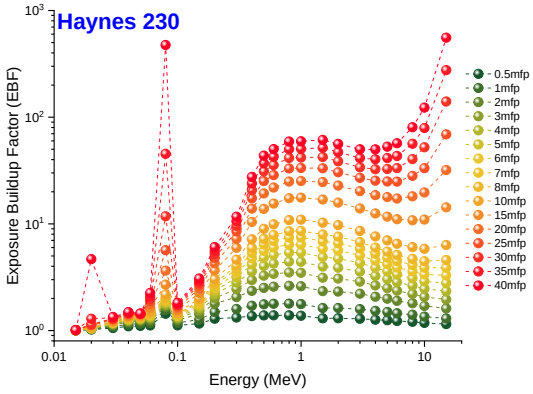

(g)

Figure 9(a-g). *Variation of exposure buildup factors (EBF) of all investigated alloy types at different mean free path values.*

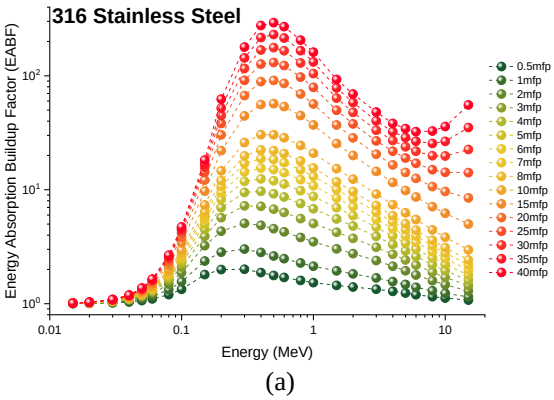

(a)

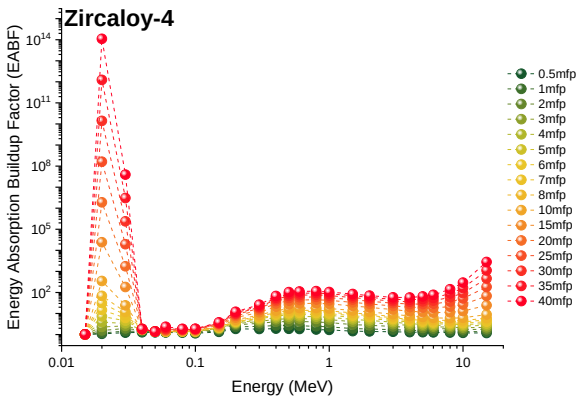

(b)

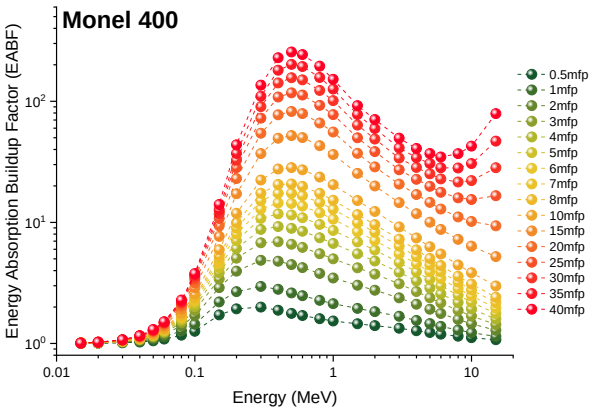

(c)

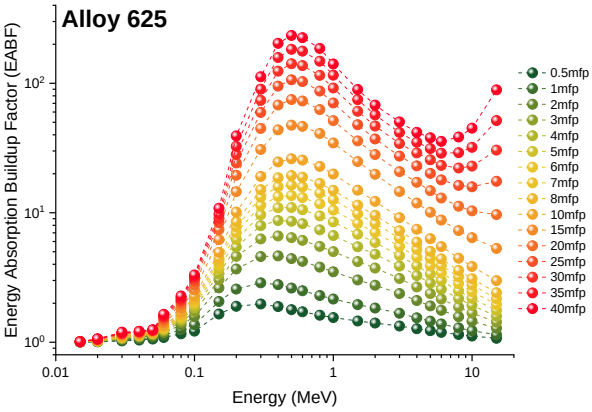

(d)

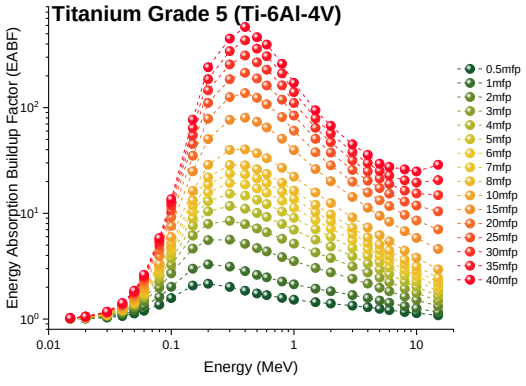

(e)

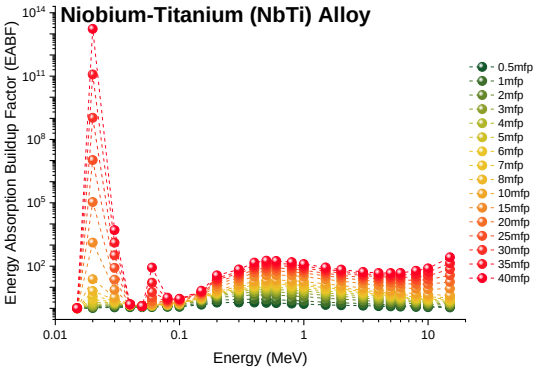

(f)

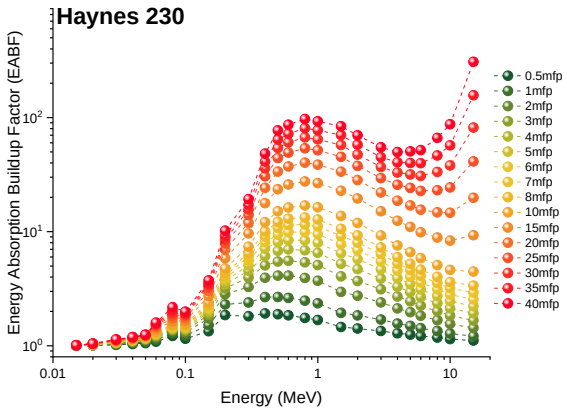

(g)

Figure 10(a-g). *Variation of energy absorption buildup factors (EABF) of all investigated alloy types at different mean free path values.*

numbers have unique peaks due to their binding energies. Within the Compton resonance zone, the EBF values remain constant, and the production of pairs causes a little increase in EBF. Among the alloys studied, the Haynes 230 alloy has the lowest EBF value, suggesting superior performance in mitigating the effects of gamma radiation compared to the other alloys. Figure 10 depicts the correlation between the energy absorption buildup factor (EABF) and the photon energy (MeV). This connection is functional for mean free paths (mfp) ranging from 5 to 40. In the last phase of the study project, the Monte Carlo MCNPX approach was used to calculate the transmission factor (TF) values for all types of alloys examined. Modifications were made to both the amounts of energy and the thicknesses of the material in order to determine the TF values. The TF values, as seen in Figure 11, exhibit an inverse correlation with the thickness of the alloy, with the values decreasing as the thickness increases. This trend remains consistent throughout a broad spectrum of energy levels and may be attributed to the proportional increase in gamma-ray absorption as the thickness of the material increases. Thicker

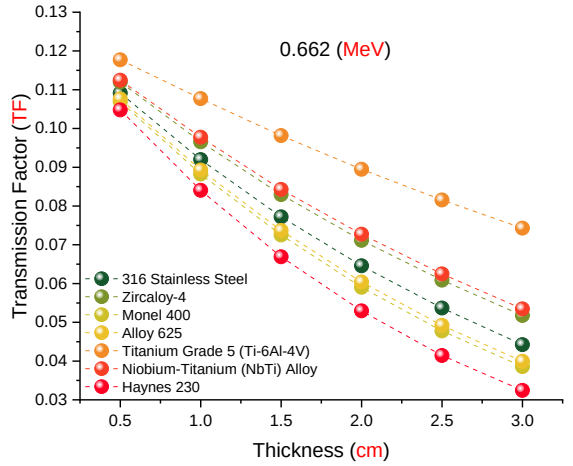

(a)

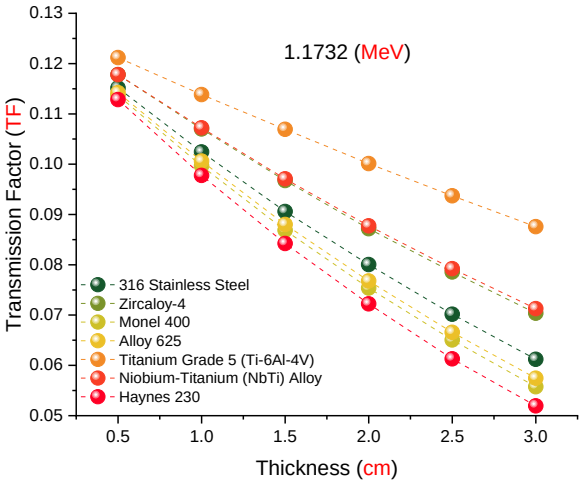

(b)

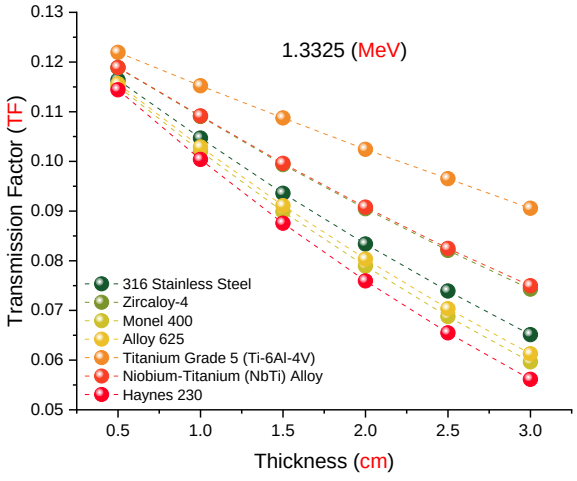

(c)

Figure 11(a-c). *Transmission Factors (TFs) of all investigated alloy types as a function of used radioisotope energy (MeV) at different alloy thicknesses.*

alloys provide more absorption, resulting in a reduction in secondary gamma-ray emission. Unlike the other alloys, the Haynes 230 alloy exhibited much higher TF values compared to the other kinds.

4. Conclusions

The objective of the research was to determine the effectiveness of seven significant alloys—316 Stainless Steel, Zircaloy-4, Monel 400, Alloy 625, Titanium Grade-5 (Ti-6Al-4V), Niobium-Titanium (NbTi) Alloy, and Haynes 230—in blocking radiation at varying energy levels and in diverse settings. The results revealed that Haynes 230 consistently showed superior performance among the investigated alloys. Haynes 230 has the highest linear attenuation coefficient and competitive mass attenuation coefficient (MAC) values, making it an excellent option for shielding against gamma radiation. Moreover, it showcased the lowest values for HVL, TVL, and mean free path (mfp), underscoring its effectiveness in minimizing the distance that radiation may travel through the material. The Fast Neutron Removal Cross Section (FNRCS) value of Haynes 230 demonstrated its superior neutron-blocking capabilities in comparison to 316 stainless steel and Monel 400. Moreover, Haynes 230 exhibited a very low exposure buildup factor (EBF), indicating its exceptional ability to effectively shield against gamma radiation. The study also examined the effective atomic number (Z_{eff}) and its relationship with photon energy, revealing that Haynes 230 has exceptional performance in gamma-ray applications. The Monte Carlo MCNPX simulations revealed that Haynes 230 exhibits the highest transmission factor (TF) values compared to all the other alloys studied, especially for thicker materials. This shows its ability to effectively absorb and reduce gamma radiation. In addition, Haynes 230's balanced performance in both gamma-ray and neutron shielding demonstrates its versatility as a radiation shield in diverse applications, ranging from nuclear reactors to radiation therapy facilities. The findings suggest that Haynes 230's combination of superior gamma attenuation, neutron shielding, and minimal buildup factor make it a strong candidate for environments with high radiation exposure, where both space efficiency and long-term material stability are critical factors. Haynes 230 is an option for radiation shielding applications because of its exceptional combination of high gamma and neutron shielding effectiveness.

Author Statements:

- **Ethical approval:** The conducted research is not related to either human or animal use.
- **Conflict of interest:** The authors declare that they have no known competing financial interests or personal relationships that could have appeared to influence the work reported in this paper
- **Acknowledgement:** The authors declare that they have nobody or no-company to acknowledge.
- **Author contributions:** The authors declare that they have equal right on this paper.
- **Funding information:** The authors declare that there is no funding to be acknowledged.
- **Data availability statement:** The data that support the findings of this study are available on request from the corresponding author. The data are not publicly available due to privacy or ethical restrictions.

References

[1] H.O.Tekin, L.R.P. Kassab, Shams A.M. Issa, C.D.S. Bordon, E.E. Altunsoy Guclu, G.R. da Silva Mattos, O. Kilicoglu (2019). Synthesis and nuclear radiation shielding characterization of newly developed germanium oxide and bismuth oxide glasses. *Ceramic International*. 45(18);24664-24674 https://doi.org/10.1016/j.ceramint.2019.08.204.

[2] Murat Aygun, Zeynep Aygun, Ercan Ercan, (2024). Newly fabricated cobalt and tungsten based alloys: Structural features and radiation protection potentials, *Nuclear Engineering and Design*, 428;113490, https://doi.org/10.1016/j.nucengdes.2024.113490.

[3] ASM International. (1990). ASM handbook, volume 1: Properties and selection: Irons, steels, and high-performance alloys. ASM International.

[4] Special Metals Corporation. (n.d.). Monel 400 technical data. Special Metals Corporation.

[5] Special Metals Corporation. (n.d.). Inconel 625: Technical data. Special Metals Corporation

[6] Special Metals Corporation. (n.d.). Nickel 200/201 technical data. Special Metals Corporation.

[7] Superconductor Materials, Inc. (n.d.). NbTi: Technical data. Superconductor Materials.

[8] Haynes International. (n.d.). Haynes 230: Technical data. Haynes International.

[9] Brookhaven National Laboratory. (n.d.). Materials handbook for fusion energy systems. Brookhaven National Laboratory.

[10] Erdem Şakar, Özgür Fırat Özpolat, Bünyamin Alım, M.I. Sayyed, Murat Kurudirek, (2020). Phy-X / PSD: Development of a user friendly online software for calculation of parameters relevant to radiation shielding and dosimetry, *Radiation Physics and Chemistry*, 166;108496, https://doi.org/10.1016/j.radphyschem.2019.108496.

[11] Shamsan S. Obaid, M.I. Sayyed, D.K. Gaikwad, Pravina.P. Pawar, (2018). Attenuation coefficients and exposure buildup factor of some rocks for gamma ray shielding applications, *Radiation Physics and Chemistry*, 148;86-94, https://doi.org/10.1016/j.radphyschem.2018.02.026.

[12] M.S. Al-Buriahi, C. Sriwunkum, H. Arslan, et al., (2020). Investigation of barium borate glasses for radiation shielding applications, *Appl. Phys. A* 126;68, https:// doi.org/10.1007/s00339-019-3254-9.

[13] Recep Kurtulus, Taner Kavas, Huseyin Ozkan Toplan, Iskender Akkurt, (2023). Highdensity and transparent boro-tellurite glass system against ionizing radiation: Fabrication and extensive characterization studies, *Ceram. Int.* 49;11, https://doi.org/10.1016/j.ceramint.2023.02.217.

[14] Maryam Yousefi, Roya Boodaghi Malidarre, Iskender Akkurt, Maria Ahmadi, Vahid Zanganeh, (2023). Physical, optical, mechanical, and radiation shielding properties for the B2O3–Li2O glasses, *Radiat. Phys. Chem.* 209;110962, https://doi. org/10.1016/j.radphyschem.2023.110962.

[15] M. Rashad, H.O. Tekin, Hesham M.H. Zakaly, Mariia Pyshkina, Shams A.M. Issa, G. Susoy, (2020). Physical and nuclear shielding properties of newly synthesized magnesium oxide and zinc oxide nanoparticles, *Nucl. Eng. Technol.* 52;9. https://doi.org/10.1016/j.net.2020.02.013.

[16] U. Kara, E. Kavaz, ShamsA.M.Issa, M. Rashad, G.Susoy, A.M.A. Mostafa, N. Yildiz Yorgun, H.O. Tekin (2020). Optical, structural and nuclear radiation shielding properties of Li2B4O7 glasses: efect of boron mineral additive. *Applied Physics A*, 126;261, https://doi.org/10.1007/s00339-020-3397-8.

[17] H.O. Tekin, V.P. Singh, T. Manici. (2017). Effects of micro-sized and nano-sized WO3 on mass attenauation coefficients of concrete by using MCNPX code *Appl. Radiat. Isot.,* 121;122-125 https://doi.org/10.1016/j.apradiso.2016.12.040.

[18] Ghada ALMisned, Duygu Sen Baykal, Hessa Alkarrani, G. Kilic, Hesham M.H. Zakaly, Shams A.M. Issa, H.O. Tekin (2024). Mechanical and, photon transmission properties of rare earth element (REE) doped BaO–B2O3–Li2O–Al2O3–P2O5 glasses for protection applications, *Journal of Radiation Research and Applied Sciences*, 17(3);101041. https://doi.org/10.1016/j.jrras.2024.101041.

[19] A.M. El-Khayatt, (2010). Calculation of fast neutron removal cross-sections for some compounds and materials, *Ann. Nucl. Energy* 37 (2); 218–222, https://doi. org/10.1016/j.anucene.2009.10.022.

[20]H.O. Tekin, Ghada ALMisned, ShamsA.M. Issa, He sham M.H. Zakaly (2022). A rapid and direct method for half value layer calculations for nuclear safety studies using MCNPX Monte Carlo code *Nucl. Eng.,Technol*., 54(9);3317-3323 https://doi.org/10.1016/j.net.2022.03.037.

[21] J. Briesmeister, MCNP—a General Monte Carlo Code for Neutron and Photon Transport, National Laboratory, Los Alamos, 2000 Report LA13709-M, version 4C.

[22] Ghada ALMisned, Hesham M.H. Zakaly, Fatema T. Ali, Shams A.M. Issa, Antoaneta Ene, Gokhan Kilic, V. Ivanov, H.O. Tekin, (2022). A closer look at the efficiency calibration of LaBr3(Ce) and NaI(Tl) scintillation detectors using MCNPX for various types of nuclear investigations, *Heliyon*, 8(10);e10839 https://doi.org/10.1016/j.heliyon.2022.e10839.

[23] Y.S. Rammah, Ashok Kumar, K. A. Mahmoud, R. El-Mallawany, F. I El-Agawany, G. Susoy, H.O. Tekin. SnO Reinforced Silicate Glasses and Utilization in Gamma Radiation Shielding Applications. *Emerging Materials Research* 9 (3);1000-1008 https://doi.org/10.1680/jemmr.20.00150.

[24] H.O. Tekin, Aly Samy Abouhaswa, O, Kilicoglu, Shams A.M. Issa, I. Akkurt, Y. Rammah. (2020). Fabrication, physical characteristic, and gamma-photon attenuation parameters of newly developed molybdenum reinforced bismuth borate glasses. *Physica Scripta* 95;115703. https://doi.org/10.1088/1402-4896/abbf6e.

[25] Yasser B. Saddeek, Shams A.M. Issa, E.E. Altunsoy Guclu, O. Kilicoglu, G. Susoy, H.O. Tekin. (2020). Alkaline phosphate glasses and synergistic impact of germanium oxide (GeO2) additive: Mechanical and nuclear radiation shielding behaviors. *Ceramics International* 46;16781-16797. https://doi.org/10.1016/j.ceramint.2020.03.254.

[26] Y.S. Rammah, H.O. Tekin, C. Sriwunkum, I. Olarinoye, Amani Alalawi, M.S. Al-Buriahi, T. Nutaro, Baris T. Tonguc. (2020). Investigations on borate glasses within SBC-Bx system for gamma-ray shielding applications. *Nuclear Engineering and Technology* 53;282-293. https://doi.org/10.1016/j.net.2020.06.034.

[27] M.S. Al-Buriahi, Halil Arslan, H.O. Tekin, V.P. Singh, Baris Tonguc. (2020). MoO3-TeO2 glass system for gamma ray shielding applications. *Mater. Res. Express* 7;025202. https://doi.org/10.1088/2053-1591/ab6db4.

[28] E.E. Altunsoy, H.O. Tekin, A. Mesbahi, I. Akkurt (2020). MCNPX Simulation for Radiation Dose Absorption of Anatomical Regions and Some Organs. *Acta Physica Polonica A* 137;4. https://doi.org/10.12693/APhysPolA.137.561.

[29] A.S. Abouhaswa, Hesham M.H. Zakaly, Shams A.M. Issa, M. Rashad, Maria Pyshkina, H.O. Tekin, R. El-Mallawany, Mostafa Y.A. Mostafa (2021). Synthesis, physical, optical, mechanical, and radiation attenuation properties of TiO2–Na2O–Bi2O3–B2O3 glasses. *Ceramics International* 47;185-204. https://doi.org/10.1016/j.ceramint.2020.08.122.

[30] Gokhan Kilic, Erkan Ilik, Shams A.M. Issa, Bashar Issa, M.S. Al-Buriahi, U. Gokhan Issever, Hesham M.H. Zakaly, H.O. Tekin (2021). Ytterbium (III) oxide reinforced novel TeO2-B2O3-V2O5 glass system: synthesis and optical, structural, physical and thermal properties. *Ceramics International* 47;18517-18531. https://doi.org/10.1016/j.ceramint.2021.03.175.

[31] E. Kavaz, H.O. Tekin, G. Kilic, G. Susoy (2020). Newly developed Zinc-Tellurite glass system: An experimental investigation on impact of Ta2O5 on nuclear radiation shielding ability. *Journal of Non-Crystalline Solids* 544;120169. https://doi.org/10.1016/j.jnoncrysol.2020.120169.

[32] M.R. Kacal, H. Polat, M. Oltulu, F. Akman, O. Agar & H.O. Tekin (2020). Gamma shielding and

compressive strength analyses of polyester composites reinforced with zinc: an experiment, theoretical, and simulation based study. *Applied Physics A* 126;205. https://doi.org/10.1007/s00339-020-3382-2.

[33] G. Lakshminarayana, Ashok Kumar, H.O. Tekin, Shams A.M. Issa, M.S. Al-Buriahi, Dong-Eun Lee, Jonghun Yoon, Taejoon Park (2020). Binary B2O3-Bi2O3 glasses: Scrutinization of directly and indirectly ionizing radiations shielding abilities. *Journal of Materials Research and Technology* 9; 14549-14567. https://doi.org/10.1016/j.jmrt.2020.10.019.

[34] A.S. Abouhaswa, Y.S. Rammah, M.I. Sayyed, H.O. Tekin (2019). Synthesis, structure, optical and gamma radiation shielding properties of B2O3-PbO2-Bi2O3 glasses. *Composites Part B* 172;218–225. https://doi.org/10.1016/j.compositesb.2019.05.040.

[35] Recep Kurtulus, Taner Kavas, Iskender Akkurt, Kadir Gunoglu, H.O. Tekin, Cansu Kurtulus (2021). A comprehensive study on novel alumino-borosilicate glass reinforced with Bi2O3 for radiation shielding applications: synthesis, spectrometer, XCOM, and MCNP-X works. *Journal of Materials Science: Materials in Electronics* 32;13882-13896. https://doi.org/10.1007/s10854-021-05964-w.

[36] M.S. Al-Buriahi, H.H. Hegazy, Faisal Alrashedi, I.O. Olarinoye, H. Algarni, H.O. Tekin, H.A. Saudi (2021). Effect of CdO addition on photon, electron, and neutron attenuation properties of boro-tellurite glasses. *Ceramics International.* 47;5951-5958. https://doi.org/10.1016/j.ceramint.2020.10.168.

[37] M.S. Al-Buriahi, Jamila S. Alzahrani, I.O. Olarinoye, Hakan Akyildirim, Sultan Alomairy, Imen Kebaili, H.O. Tekin and Chalermpon Mutuwong (2021). Role of heavy metal oxides on the radiation attenuation properties of newly developed TBBE-X glasses by computational methods. *Physica Scripta* 96;075302. https://doi.org/10.1088/1402-4896/abf86a.

[38] Kurtulus, R., Kavas, T., Akkurt, I., Günoğlu, K., Tekin, H. O., & Kurtulus, C. (2021). A comprehensive study on novel alumino-borosilicate glass reinforced with Bi2O3 for radiation shielding applications: Synthesis, spectrometer, XCOM, and MCNP-X works. *Journal of Materials Science: Materials in Electronics*, 32;13882-13896. https://doi.org/10.1007/s10854-021-05964-w

[39] Al-Buriahi, M. S., Hegazy, H. H., Alrashedi, F., Olarinoye, I. O., Algarni, H., Tekin, H. O., & Saudi, H. A. (2021). Effect of CdO addition on photon, electron, and neutron attenuation properties of boro-tellurite glasses. *Ceramics International* , 47, 5951-5958. https://doi.org/10.1016/j.ceramint.2020.10.168

[40] Al-Buriahi, M. S., Alzahrani, J. S., Olarinoye, I. O., Akyildirim, H., Alomairy, S., Kebaili, I., Tekin, H. O., & Mutuwong, C. (2021). Role of heavy metal oxides on the radiation attenuation properties of newly developed TBBE-X glasses by computational methods. *Physica Scripta* , 96, 075302. https://doi.org/10.1088/1402-4896/abf86a

[41] Şen BAYKAL, D. (2024). A novel approach for Technetium-99m radioisotope transportation and storage in lead-free glass containers: A comprehensive assessment through Monte Carlo simulation technique. *International Journal of Computational and Experimental Science and Engineering*, *10*(2);102-111. https://doi.org/10.22399/ijcesen.304

[42] KUTU, N. (2024). Gamma ray Shielding Properties of the 57.6TeO2-38.4ZnO-4NiO system. *International Journal of Computational and Experimental Science and Engineering*, *10*(2);141-145. https://doi.org/10.22399/ijcesen.31

[43] KAYAHAN, S. H., KUTU, N., & GUNAY, O. (2024). Radiation Dose Levels in Submandibular and Sublingual Gland Regions during C-Arm Scopy. *International Journal of Computational and Experimental Science and Engineering*, *10*(2);168-173. https://doi.org/10.22399/ijcesen.320

[44] KUTU, N. (2024). Neutron Shielding Properties of Cellulose Acetate CdO-ZnO Polymer Composites. *International Journal of Computational and Experimental Science and Engineering*, *10*(2);203-206. https://doi.org/10.22399/ijcesen.322

[45] CENA, B., & HASI, N. (2024). Handling of radioactive waste from the use of radionuclides in hospitals. *International Journal of Computational and Experimental Science and Engineering*, *10*(2);207-214. https://doi.org/10.22399/ijcesen.331

[46] Karpuz, N. (2024). Effective Atomic Numbers of Glass Samples. *International Journal of Computational and Experimental Science and Engineering*, *10*(2);236-240. https://doi.org/10.22399/ijcesen.340

[47] Cena, B. (2024). Determination of the type of radioactive nuclei and gamma spectrometry analysis for radioactive sources. *International Journal of Computational and Experimental Science and Engineering*, *10*(2);241-246. https://doi.org/10.22399/ijcesen.321